Monte Carlo calculated wall and axial non-uniformity corrections for primary standards of air kerma

D.W.O. Rogers and J. Treurniet
Ionizing Radiation Standards
National Research Council of Canada
Ottawa, K1A OR6

May 1999

NRCC Report PIRS-663

This report, including the appendices, is available on-line at:
http://www.irs.inms.nrc.ca/inms/irs/papers/PIRS663/pirs663.html

Abstract

Following the approach of an earlier NRC paper[1], this report uses improved Monte Carlo techniques to recalculate the wall attenuation and scatter corrections, K_{wall}, and axial non-uniformity corrections, K_{an}, for a wide range of ion chambers which are the primary standards of air kerma for their respective national metrological institutes (NMIs). It is first demonstrated that the Monte Carlo calculations are capable of reproducing the experimental data upon which the standards laboratories have based their values of K_{wall}, in the majority of cases, well within 0.2%. The calculated correction factors are then systematically applied to all chambers and the results of many international comparisons of air kerma rates determined by the NMIs to that determined by the BIPM are revised. This is done for 16 chambers for ^{60}Co beams and for 5 chambers for ^{137}Cs beams. In the ^{60}Co beams the mean value of the measured air-kerma rate increases by 0.8% while the rms deviation of the results increases from 0.2% to 0.3%, with most of the increase in the scatter due to just 3 laboratories. The results for the ^{137}Cs beam are less clear cut, but the revised values show no more spread than the original data. If one considers just the chamber type recently analyzed by Boutillon[2] it is shown that using the calculated correction factors significantly improves the original results which she found inconsistent.

Contents

1 Introduction

In earlier NRC papers it has been argued that the standard linear extrapolation technique for obtaining wall attenuation and scatter corrections for primary standards is incorrect[1, 3, 4]. The argument is based on using the Monte Carlo techniques to calculate explicitly the wall correction factors[5, 6] by scoring the energy deposited less the effects of attenuation and scatter and comparing this to the total energy deposited. The techniques used to calculate the removal of the attenuation and scatter techniques are based on a rigorous analysis[3, 7]. The Monte Carlo calculations were shown to agree with much of the available experimental data on wall attenuation measurements and yet they predicted a correction factor which was very different from the extrapolated values used to determine the primary standards. Using a highly simplified model, Bielajew showed, for the case of photons incident on the curved surface of an ion chamber, that the proper extrapolation to zero wall thickness was non-linear[4] and that in fact the analytic non-linear extrapolation theory predicted the same results as obtained using the direct Monte Carlo calculation. This theory doesn't apply to pancake type chambers, and in this case the Monte Carlo calculations imply the non-linearity actually causes the wall attenuation correction to be smaller than obtained from extrapolation to zero wall thickness. As shown in our previous report to the CCEMRI(I)[8] and presented at an AAPM meeting[9], Shortt *et al.* have done a series of measurements with a thin-walled graphite chamber in a ^{137}Cs beam and have shown the extrapolation is non-linear as predicted by Bielajew's analytic theory and the Monte Carlo calculations.

Despite the fairly convincing theoretical, calculational and experimental results, few standards laboratories have moved away from the linear extrapolation technique. However various groups have begun to do so, either directly or indirectly. The NPL calculates its overall correction factors using Monte Carlo techniques and has confirmed that their "effective wall correction factor" is equivalent to the directly calculated Monte Carlo results (Simon Duane, private communication, 1999). The LPRI calculates its wall correction factors using an extrapolation technique which is non-linear to take into account that the side wall of their chamber does not change its effective thickness linearly[10]. At NRC we use the directly calculated Monte Carlo results.

As well as the problems related to wall corrections, there has been some debate over the correction for axial non-uniformity or the point of measurement correction. In this case most standards laboratories use $K_{\mathrm{an}} = 1.000$ but a few major labs use corrections which are significantly different from unity (in particular the BIPM and the PTB). In a major theoretical paper, Bielajew extended the work of Kondo and Randolph[11] to include anisotropic electron effects within an analytic theory[12, 13]. This theory is capable of explaining measured data for sources very close to ion chambers[14]. The theory predicts K_{an} factors which are very close to unity for chambers at 1 m from a ^{60}Co source. By using Monte Carlo techniques, Bielajew and Rogers[1] have also confirmed the predictions of this theory for the NRC and BIPM chambers by quite literally running the calculation for weeks.

In a 1992 paper, Bielajew and Rogers examined the implications of both of these changes if they were systematically made to 7 different primary standards for air kerma. The result was to raise the mean air kerma rate by 0.64% although the spread in values did not change significantly (from 0.66% to 0.67%). As it happens, the NRC and BIPM standards went from being near the average to being the two lowest standards for air kerma.

In the last few years there have been significant improvements in our ability to do accurate and high precision ion chamber calculations. The first important step is the development of a new generation of EGS code, called EGSnrc, which is capable of calculating ion chamber response with an accuracy of 0.1% or so (relative to its own cross-sections)[15, 16]. A second major step is the increase in computing power available, and the ease with which Monte Carlo calculations can be run on multiple CPUs (we use up to 38 machines for a single calculation). Given these advances, we have undertaken to recalculate the K_{wall} and K_{an} corrections for all of the primary standards for which we can get adequate information. Because of the increase in computing power we can do these calculations using a much more direct approach than in the past. Furthermore, with the calculations of K_{wall} we systematically show that the Monte Carlo calculations agree at the 0.1 to 0.2% level with all the experimental data available.

Our goals are to present calculated values for K_{wall} and K_{an} correction factors for all primary standards for which we have adequate information, to demonstrate the ability of the Monte Carlo calculations to predict accurately the value of K_{wall} obtained by extrapolation, and then to update the revision of Bielajew and Rogers to all of the current key comparison data.

2 Theory

The basic equation for air kerma is given by:

$$K_{\mathrm{air}} = \left(\frac{W}{e}\right)_{air} \frac{Q_{gas}}{m_{air}(1-g)} \left(\frac{\overline{L}}{\rho}\right)_{\mathrm{air}}^{\mathrm{wall}} \left(\frac{\overline{\mu_{\mathrm{en}}}}{\rho}\right)_{\mathrm{wall}}^{\mathrm{air}} K_{\mathrm{h}} K \qquad [\mathrm{Gy}], \tag{1}$$

where the symbols have their normal meanings[17] and K is the product of many correction factors. In this paper we are concerned with the following factors:

$$K = K' K_{\mathrm{wall}} K_{\mathrm{an}} \tag{2}$$

where K_{wall} corrects for attenuation and scatter of photons in the walls of the ion chamber and K_{an} corrects for the fact that we measure in a beam from a point source but the theory assumes a parallel beam. The factor K' contains many other effects which are important, but not the subject of this paper. Note in particular that there is a correction factor, K_{rn} which accounts for radial non-uniformity which, in principle, includes a component related to the point source correction. However, it has been shown that the radial non-uniformity due to the strict point source aspects of the beam is negligible compared to issues such as collimator scatter and general non-uniformity of the beam[1] and thus K_{rn} is not considered here.

The wall correction factor is often split up into 3 factors by various laboratories and is written:

$$K_{\mathrm{wall}} = K_{\mathrm{at}} K_{\mathrm{sc}} K_{\mathrm{cep}} \tag{3}$$

The traditional way to evaluate K_{wall} is to measure the ion chamber response as a function of wall thickness as additional wall material is added to the chamber on all sides and then to extrapolate linearly to zero wall thickness. The value obtained this way is then multiplied by a calculated value for K_{cep} which accounts for the fact that the center of electron production is upstream of where the energy is deposited.

The factor K_{an} is determined in different ways. There are two traditional approaches. One approach is to take the center of the chamber as the effective point of measurement because of the symmetries of the situation. This implies $K_{\mathrm{an}} = 1.000$. A second method (used by the BIPM, the PTB[18, 19] and others, see table 5) is to calculate the correction and this leads to K_{an} values up to 0.75% less than unity.

3 Calculations

The Monte Carlo calculations are done using a new version of EGS4[20] which is called EGSnrc because it is a massive reworking of the code[15, 16]. It has been shown to calculate ion chamber response with an accuracy of 0.1% or better (relative to its own cross-sections). This code is undergoing extensive benchmarking within NRC at present. The calculations of K_{wall} and ion chamber response are done using the NRC user-codes CAVRZnrc and CAVSPHnrc for cylindrical and spherical chambers respectively. These codes calculate K_{wall} using the unweighting method described in detail previously[3, 7]. Kawrakow has demonstrated that these methods work by calculating K_{wall} by regenerating any photons which interact and by immediately discarding any scattered photons[16]. Bielajew has also formally proven the equivalence of these two methods[13].

In the past K_{an} was calculated analytically for various chambers using the techniques of Bielajew[12] and calculated within CAVRZ using a correlated sampling technique[13]. In the present paper we go back to the fundamental definition and calculate K_{an} as:

$$K_{\mathrm{an}} = \frac{D_{\mathrm{gas}}^{\mathrm{parallel}} K_{\mathrm{wall}}^{\mathrm{parallel}}}{D_{\mathrm{gas}}^{\mathrm{point}} K_{\mathrm{wall}}^{\mathrm{parallel}}} \tag{4}$$

where D_{gas} is the calculated dose to the cavity gas per incident unit fluence for a parallel or point source beam and K_{wall} is the wall attenuation and scatter correction in the same cases. This approach is taken because it requires no complex scoring routines and provides a very straight forward approach to what we mean by K_{an}. To obtain high precision for this calculation requires considerable computing power (typically more than 100 hours of CPU time (Pentium Pro 200 MHZ) per calculation). The results are consistent with both the previous analytic calculations by Bielajew[12] and the previous Monte Carlo calculations using correlated sampling[1].

In a previous paper it was shown that the Monte Carlo calculations were in good agreement with the wall extrapolation data available from several standards laboratories. This was done by calculating K_{wall} for each chamber thickness and then making use of the fact that the overall response was proportional to K_{wall}^{-1}. This was done because the statistical precision on K_{wall} is much better than on the overall calculated chamber response. In the present work we can avoid this approach and calculate the chamber response directly as a function of wall thickness. After doing this for a range of thicknesses, we extrapolate linearly back to zero wall thickness and compare the value obtained this way to that obtained experimentally for those chambers where linear extrapolation is used. This generally can be done only for chambers with all walls of equal thickness. In the case of the BIPM chamber a more complex extrapolation technique is used for each wall separately and we model these experiments explicitly.

We use as realistic a model of the ion chambers as possible within the restrictions of cylindrical or spherical symmetry. This includes modelling the insulators and electrodes. The dimensions are contained in table 1. In the case of the LPRI chamber which is cylindrical with hemispherical ends, we cannot model this geometry so we model it as two limiting cases as a sphere or a cylinder with the same volume. In the Monte Carlo calculations we use a realistic bulk density for each chamber but we use the density effect corresponding to the crystalline density of graphite because the recently measured stopping powers of graphite are found to agree with the ICRU values using the crystalline density[21].

In the calculations we use a ^{60}Co photon spectrum taken from the literature[22]. It is the on-axis photon spectrum calculated from a detailed Monte Carlo model of a ^{60}Co unit. In some of the previous work done at NRC we have used a mono-energetic spectrum. This causes a difference in calculated $K_{\rm wall}$ factors of about 0.2%, which is now clearly visible in the calculations which have better statistical precision than previously[1].

The calculations are done for a point source at 100 cm from the mid-point of the chamber. The electrons are followed down to 10 keV kinetic energy and the photons to 1 keV.

4 Results

4.1 Comparison to extrapolated wall data for ^{60}Co beams

The values of $K_{\rm at}K_{\rm sc}$ obtained from Monte Carlo calculations by extrapolating to zero wall thickness are presented in Table 2 and compared to the experimental results presented in various reports (listed in the table). Individual graphs showing the calculated response vs. wall thickness and the extrapolation are shown in the appendix . This method can only be applied to chambers for which all walls are equal.

The Monte Carlo calculated and measured data in table 2 are generally in good agreement. The worst discrepancies are for the VNIIM chambers for which we have little information and, surprisingly, the differences are in opposite directions for the two chambers. For all other chambers the calculated values are within 0.15% of the linearly extrapolated values except for the LPRI chamber where the two approximate geometries modelled give results which bracket the measured values.

Figure 1 and table 3 present comparisons to the BIPM experimental extrapolation data which show similar very good agreement with the measurements.

4.2 Calculated ^{60}Co $K_{\rm wall}$ and $K_{\rm an}$ values compared to those used

Table 6 presents a comparison of the Monte Carlo calculated value of $K_{\rm wall}$ and the value used by each standards laboratory for ^{60}Co beams. Here the discrepancies are generally much larger than in table 5 where the agreement with the actual extrapolation data was generally good. In the case of $K_{\rm wall}$ the disagreement is much worse, ranging from +1% for spherical and near-spherical cylindrical chambers, to around 0 for thimble chambers , to −0.4% for a pancake chamber. These results are similar to the previously reported results[1] except the present study covers a larger range of standard chambers.

In the case of $K_{\rm an}$ the results are mixed, depending on which theory was previously used. Many labs have correctly used a value very close to 1.0 which the calculations explicitly show to be correct. In some other cases though the disagreement is much more substantial, leading to differences of up to 0.9% in one case.

4.2.1 Changes related to the BIPM standard

The BIPM standard has undergone some changes since the paper of Bielajew and Rogers was published[1]. In 1996 the BIPM reported some changes in the correction factors because of a change in the source, which increased the scatter component of the beam significantly, and they moved from a calibration point at 112 cm to one at 100 cm[23]. These changes, along with the improved statistics on our present calculations, lead to a change in what the effects of using the Monte Carlo calculated results instead of the BIPM's original corrections.

Thus, in 1973 the BIPM reported $K_{\rm wall} = 1.0037(12)$ and $K_{\rm an} = 0.9968(10)$[19]. In 1996 and thereafter they reported their standard was based on $K_{\rm wall} = 1.0028$ and $K_{\rm an} = 0.9964(7)$.

In the 1992 paper, NRC's estimates of the BIPM's values were $K_{\rm wall} = 1.0008(6)$ and $K_{\rm an} = 1.0022$[1]. These values implied that the BIPM standard would change by +0.25% if the NRC corrections were applied. The present calculations give $K_{\rm wall} = 1.00139(3)$ (which is the same as before within the previous statistics) and $K_{\rm an} = 1.0024(3)$, again the same. Thus using our present improved results for older comparisons, the BIPM standard would change by +0.33% and for comparisons based on the new standard, the BIPM standard would change by +0.46%.

4.3 Revision of the ^{60}Co comparison results

If, as previously[1], we apply the Monte Carlo calculated correction factors for both the NMI and the BIPM for each of the reported comparisons, we can determine a revised set of comparison results. We have not adjusted the uncertainties. We include the BIPM in the analysis as 1.000 with an uncertainty of 0.17%[24] (this provides a worst case result for the arguments here). The revised results are shown in table 6. The one complication is that comparisons are done with the BIPM standard using different values of $K_{\rm wall}$ and $K_{\rm an}$ and hence we must keep track of that when making the revisions. The revised results are shown and compared to the original data in figure 2 and a statistical analysis presented in Table 7. Visually the revised data are reasonably consistent. Table 7 shows that the rms deviation of the results is 0.32% for the revised data compared to 0.19% for the original data. The χ^2 values are significantly worse for the revised data, but still acceptable with a p value of 0.08. The table shows that almost all of the problem in the χ^2 value comes from the VNIIM result, which has one of the smaller reported uncertainties and the BIPM result which has the smallest reported uncertainty. If we exclude either of these results the p value goes to about 0.4 and if we exclude both results it goes to 0.90.

The most dramatic conclusion is that the revision implies that the average air-kerma rate must be increased by 0.8% (+0.48% from the weighted mean less the original 0.16% from the weighted mean +0.46% from the change in the BIPM standard itself for the latest values of K_{wall} and K_{an} used by the BIPM).

4.4 Exploratory results regarding ^{137}Cs comparisons

Some calculations are done for a set of chambers used in ^{137}Cs beam comparisons[2, 25]. Tables 8 and 9 present comparisons of the Monte Carlo calculated and original values of K_{wall} and K_{an} for various chambers in a ^{137}Cs beam. The change in K_{wall} is the same as in the ^{60}Co beam case for the spherical and pancake chambers and is slightly larger for the large cylindrical CC01 chambers. On the other hand, the change in K_{an} for the BIPM pancake chamber is less than in the ^{60}Co beam. This is due to a change in the value evaluated at the BIPM, the Monte Carlo calculated K_{an} does not change within the uncertainties.

Table 10 shows the effects for selected chamber of applying the NRC calculated K_{wall} and K_{an} correction factors. Here the results are not as complete nor as clear cut as in the ^{60}Co case. There is much more scatter in the original results and this remains after the revisions, although the average value has increased in this case by about 0.8% as well.

If we concentrate on just those chambers also considered by Boutillon recently[2] (chambers 1 to 4 in the figures), it becomes clear that the revision causes the data to be much more consistent than the original data, although the average goes from being considerably less than 1.0 to being somewhat higher than 1 (shown by the solid lines in the figures).

4.5 Why do the results look so different from those of Boutillon?

Boutillon has recently done a similar sort of analysis but restricted to comparisons between the BIPM chamber and the CC01 chambers (SZMDM, UDZ, LNMRI, GUM, OMH, BEV, BIPM)[2]. In her analysis of the ^{60}Co beams she finds that after adjusting the comparison results to use the calculated values of K_{wall} and K_{an}[1], there is more than an 0.7% difference between the average for the results for the 9 CC01 chambers and the BIPM pancake chamber. For the 5 cases we have here, the average is a difference of 0.48%. However, one gets a different perspective when the other types of chambers are included and sees that the BIPM result is one of the extremes of the distribution, along with the NRC chamber. The statistical

[1] she actually uses a terminology that includes K_{an} in K_{wall}

analysis in section 4.3 demonstrates that the subset of chambers used by Boutillon was giving a distorted picture, and on a purely statistical basis there is no way to chose between the alternatives.

For the ^{137}Cs comparisons, Boutillon was forced to conclude that something was wrong but she had no data for correcting the $K_{\rm wall}$ and $K_{\rm an}$ factors. As seen in the previous section, for just the chambers that she considered, the Monte Carlo calculated values of $K_{\rm wall}$ and $K_{\rm an}$ provide a solution to the problem. However, if one also considers the NIST standard the results look as troublesome as using the original results.

5 Summary and Conclusions

We have repeated the earlier analysis of Bielajew and Rogers[1] using higher precision Monte Carlo data and a wider selection of standards. Furthermore, we have demonstrated that in almost all cases we can reproduce the measured experimental data on wall attenuation within 0.1 to 0.2%. The results indicate that using the Monte Carlo calculated results for $K_{\rm wall}$ and $K_{\rm an}$ provides a consistent set of comparison results for ^{60}Co beams. The variation between standards has increased, but the increase is not statistically significant and is due almost entirely to the standards of 2 laboratories. At the same time the average value of the absolute air-kerma scale has increased by about 0.8%. Roughly the same increase is seen in the average ^{137}Cs air-kerma rate if the Monte Carlo calculated values of $K_{\rm wall}$ and $K_{\rm an}$ are used. The Monte Carlo results for ^{137}Cs beams explain the discrepancies noted by Boutillon[2] but introduce others when other chambers are considered.

6 Acknowledgments

This work was partially supported by NIH grant No RO1-CA66852.

7 Tables

Table 1: The standards. For the PTB chambers, the electrode dimensions were not given, so they were estimated based on the volume given.

Lab	shape	ρ ($g\ cm^{-3}$)	Inner radius (cm)	Outer radius (cm)	Radial wall thickness (cm)	Inner length (cm)	Outer length (cm)	Planar wall thickness (cm)	Electrode diameter/length (cm)	Insulator type
GUM	cyl	1.71	0.55	0.95	0.4	1.1	1.9	0.4	0.2/1.	none
LNMRI	cyl	1.71	0.55	0.95	0.4	1.1	1.9	0.4	0.2/1.	polyethylene
IRD	cyl	1.71	0.55	0.95	0.4	1.1	1.9	0.4	0.2/1.	polyethylene
SZMDM	cyl	1.75	0.55	0.95	0.4	1.1	1.9	0.4	0.2/1.	polyethylene
UDZ	cyl	1.75	0.55	0.95	0.4	1.1	1.9	0.4	0.2/1.	polyethylene
OMH	cyl	1.75	0.55	0.95	0.4	1.1	1.9	0.4	0.2/0.897	PTFE (Teflon)
ENEA	cyl	1.75	0.55	0.95	0.4	1.1	1.9	0.4	0.2/0.897	PTFE (Teflon)
VNIIM	C1, cyl	1.634	0.5535	0.9535	0.4	0.5530	1.3530	0.4	0.198/0.795	polyethylene
	C30, cyl	1.634	1.605	2.005	0.4	3.70	4.50	0.4	0.2/2.59	PTFE (Teflon)
BIPM	pancake	1.84	2.25	2.525	0.275	0.513	1.079	0.283	4.0982/0.10195	none
NIST[b])	30 cm^3 sph	1.74	1.9284	2.3035	0.3751	N/A	N/A	N/A	N/A	none
	50 cm^3 sph	1.73	2.3048	2.67	0.3652	N/A	N/A	N/A	N/A	none
PTB(a)	cyl	1.73	0.3	0.6	0.3	2.0	2.7	0.35	0.1/0.62	none
PTB(b)	cyl	1.73	0.5	0.8	0.3	2.0	2.7	0.35	0.1/1.394	none
PTB(c)	pill-box	1.72	2.2	2.6	0.4	0.45	1.25	0.4	3.9166/0.05	none
NMi	sph	1.8045	1.05	1.45	0.4	N/A	N/A	N/A	N/A	none
NRC3C	cyl	1.66	0.7919	1.175	0.383	1.6135	2.5255	0.456	0.6704/1.2002	polystyrene
ARL	pancake	1.73	2.25115	2.52325	0.2721	0.51501	10.7918	2.8139/2.8278	4.10132/1.002	none
LPRI	cyl[a]	1.80	1.1	1.4	0.3	2.5667	3.1667	0.3	0.2/2.2	none
LPRI	sph[a]	1.80	1.32558	1.62558	0.3	N/A	N/A	N/A	0.50916/N/A	none

[a] LPRI is a cylinder with two hemispheres. We have approximated it to a sphere and to a cylinder of equivalent chamber and electrode volumes.
[b] The radii were in error in the original report, but the calculations were done with the values shown here.

Table 2: Comparison of the Monte Carlo values of $K_{at}K_{sc}$ obtained by extrapolating the response to zero wall thickness, with those reported by the BIPM and other sources. The SZMDM and UDZ values are calculated from the reported K_{wall} values using K_{cep}=0.997. The two BIPM values are from 1973[19] and 1996[23]. Here and elsewhere, one standard deviation uncertainties in the last digit are shown in brackets at the end of each number.

Lab	$K_{at}K_{sc}^{extrap}$ Monte Carlo	$K_{at}K_{sc}$ "measured"	ref	%Δ
GUM	1.0161(7)	1.0155(10)	[26]	0.059
LNMRI	1.0167(9)	1.0155(8)	[27]	0.118
SZMDM	1.0165(2)	1.0154(9)	[28]	0.108
UDZ	1.0165(2)	1.0161(12)	[29]	0.039
OMH	1.0164(12)	1.0157(7)	[30]	0.069
ENEA	1.0164(12)	1.0156(5)	[31]	0.079
VNIIM C1	1.0148(8)	1.0120(15)	[32]	0.276
VNIIM C30	1.0155(1)	1.0190(15)	[32]	-0.344
BIPM	[a]	1.0114(23)	[18]	
		1.0107(7)	[27]	
NIST-30	1.0235(8)	1.0220	[33]	0.147
NIST-50	1.0242(5)	1.0227	[33]	0.147
PTB(a)	[b]	1.0122(5)	[19]	
PTB(b)	[b]	1.0127(10)	[19]	
PTB(c)	1.0110(2)	1.0098(20)	[19]	0.119
NMi	1.0243(8)	1.023(1)	[c]	0.127
LPRI cyl	1.0133(1)	1.016	[d]	-0.266
LPRI sph	1.0173(4)	1.016	[d]	0.128

[a] The BIPM does not use this extrapolation method; see Table 3 for a summary of data measured by the BIPM compared to Monte-Carlo simulation.
[b] The PTB(a) and (b) chambers do not have uniform wall thickness, hence the extrapolation method cannot be applied.
[c] private comminication, Jan Bultman, 1989.
[d] private communication, J.P. Simoën, May 1993. This is their value for a linear extrapolation of their measured data.

Table 3: Comparison of the BIPM extrapolation data reported by Boutillon and Niatel[18] to data obtained by Monte Carlo simulation (see also fig 1). The front wall extrapolation is fit to both a parabola of the form $y = a + bx + cx^2$ (since this is what the BIPM did[18]) and to a straight line, $y = a + bx$. Note that the uncertainty in the extraplolation with the parabola is very large. The back and side walls are fit to a straight line.

Wall	Deviation from unity	BIPM deviation
Front		
parabola	1.58(53)%	1.85%
line	1.94(1)%	1.85%
Back	0.29(1)%	0.18%
Side	0.26(2)%	0.39%

Table 4: Comparison of the Monte Carlo $K_{\rm wall}$ values obtained with EGSnrc with those reported by BIPM and other sources. The two BIPM values are from 1973 and 1996.

Lab	$K_{\rm wall}^{\rm MC}$	$K_{\rm wall} = K_{\rm at}K_{\rm sc}K_{\rm cep}$	ref	%Δ
GUM	1.02106(5)	1.0109(14)	[26]	0.980
LNMRI	1.02111(5)	1.0125(13)	[27]	0.847
SZMDM	1.02157(5)	1.0124(9)	[28]	0.902
UDZ	1.02157(5)	1.0131(12)	[29]	0.833
OMH	1.02190(5)	1.0127(7)	[30]	0.909
ENEA	1.02190(5)	1.0127(21)	[31]	0.904
VNIIM C1	1.02007(7)	1.0090(15)	[32]	1.091
VNIIM C30	1.02956(5)	1.0154(15)	[32]	1.385
BIPM	1.00139(3)	1.0037(23)	[18]	-0.230
		1.0028(8)	[27]	-0.141
NIST-30	1.02710(4)	1.0169(10)	[33]	0.998
NIST-50	1.02740(5)	1.0176(10)	[33]	0.958
PTB(a)	1.00936(7)	1.0092(16)	[19]	0.016
PTB(b)	1.01274(4)	1.0097(18)	[19]	0.301
PTB(c)	1.00275(3)	1.0068(25)	[19]	-0.403
NMi	1.02607(3)	1.0179(22)	[a]	0.799
NRC3C	1.02239(7)	1.0218(5)[b]		0.058
ARL	1.00100(4)	0.9987(19)	[24]	0.230
LPRI cyl	1.02441(7)	1.0152(21)	[34]	0.903
LPRI sph	1.02102(4)	1.0152(21)	[34]	0.572

[a] private communication, Jan Bultman, 1989.

[b] Most of the change is due to the use of a spectrum rather than mono-energetic incident photons.

Table 5: Comparison of the Monte Carlo K_{an} axial non-uniformity values obtained with EGSnrc with those reported by BIPM and other sources. The two BIPM values are from 1973 and 1996. The Monte Carlo values are calculated by dividing the parallel beam value by the point source value.

Lab	dose$\times K_{wall}^{MC,point}$ $\times 10^{-12}$Gy	dose$\times K_{wall}^{MC,parallel}$ $\times 10^{-12}$Gy	K_{an}^{MC}	K_{an}^{NMI}	ref	%Δ
GUM	4.5677(14)	4.5667(14)	0.9998(4)	1.0000(1)	[26]	-0.020
LNMRI	4.5626(18)	4.5611(18)	0.9997(6)	1.0000(7)	[27]	-0.030
SZMDM	4.5637(14)	4.5647(18)	1.0002(5)	0.997(1)	[28]	0.320
UDZ	4.5637(14)	4.5647(18)	1.0002(5)	0.9998(10)	[29]	0.040
OMH	4.5724(14)	4.5718(14)	0.9999(4)	0.9998(10)	[30]	0.010
ENEA	4.5724(14)	4.5718(14)	0.9999(4)	0.997(1)	[31]	0.290
VNIIM C1	4.5634(14)	4.5634(18)	1.0000(5)	0.9998(5)	[32]	0.020
VNIIM C30	4.5665(9)	4.5707(9)	1.0009(3)	0.9996(5)	[32]	0.130
BIPM	4.5556(14)	4.5667(5)	1.0024(3)	0.9968(20)	[18]	0.560
				0.9964(7)	[27]	0.600
NIST-30	4.5671(5)	4.5691(5)	1.0004(1)	1.0000(2)	[33]	0.040
NIST-50	4.5699(9)	4.5692(9)	0.9998(3)	1.0000(2)	[33]	-0.020
PTB(a)	4.5626(9)	4.5673(18)	1.0010(4)	0.9955(15)	[19]	0.551
PTB(b)	4.5662(9)	4.5671(5)	1.0002(2)	0.9925(15)	[19]	0.773
PTB(c)	4.5554(9)	4.5678(14)	1.0027(4)	0.9933(15)	[19]	0.942
NMi	4.5658(14)	4.5666(9)	1.0002(4)	1.0000(36)		0.020
NRC3C	4.5445(14)	4.5473(9)	1.0006(4)	0.9999(4)		0.070
ARL	4.5544(9)	4.5648(9)	1.0023(3)	0.9963	[24]	0.600
LPRI cyl	4.5689(9)	4.5687(9)	1.0000(2)	1.0000(5)	[34]	0.000
LPRI sph	4.5661(14)	4.5648(14)	0.9997(4)	1.0000(5)	[34]	-0.030

Table 6: Revised values of ^{60}Co comparison results after correcting both the NMI and BIPM air-kerma rates to use the Monte Carlo calculated values of K_{wall} and K_{an}. There are no adjustments of the uncertainties.

Lab	$\left(\frac{K_{\mathrm{lab}}}{K_{\mathrm{BIPM}}}\right)_{\mathrm{orig}}$	ΔK_{wall}	ΔK_{an}	$\left(\frac{K_{\mathrm{lab}}}{K_{\mathrm{BIPM}}}\right)_{\mathrm{revised}}$	$K_{\mathrm{wall}}^{\mathrm{BIPM}}$
GUM	0.9987(28)	1.00980	0.99980	1.0037(28)	1.0028
LNMRI	1.0004(23)	1.00847	0.99970	1.0040(23)	1.0028
SZMDM	0.9982(19)	1.00902	1.00320	1.0058(19)	1.0028(assumed)
UDZ	0.9992(23)	1.00833	1.00040	1.0033(23)	1.0028(assumed)
OMH	1.0025(24)	1.00909	1.00010	1.0071(24)	1.0028(assumed)
ENEA	1.0017(35)	1.00904	1.00290	1.0091(35)	1.0028(assumed)
VNIIM C30	1.0020(28)	1.01385	1.00130	1.0126(28)	1.0028
BIPM (1973)	1.0000	0.99770	1.00560	1.0000	1.0037
(1996)	1.0000	0.99859	1.00600	1.0000	1.0028
NIST[a]	0.9980(40)	1.00978	1.00010	1.0033(40)	1.0028
PTB(a)	1.0020(49)	1.00016	1.00551	1.0044(49)	1.0037
PTB(b)	0.9991(46)	1.00301	1.00773	1.0065(46)	1.0037
PTB(c)	1.0040(45)	0.99597	1.00942	1.0061(45)	1.0037
NMi	1.0031(37)	1.00799	1.00020	1.0067(37)	1.0028
NRC3C	1.0020(40)	1.00058	1.00070	0.9987(40)	1.0028
ARL	1.0028(32)	1.00230	1.00600	1.0065(32)	1.0028
LPRI cyl	1.0025(26)	1.00903	1.00000	1.0069(26)	1.0028
LPRI sph	1.0025(26)	1.00572	0.99970	1.0033(26)	1.0028

[a]averaging the changes for the two chambers.

Table 7: Statistics involved in determining the mean value of the original and revised air-kerma comparison data for ^{60}Co. The third column shows the revised data without the VNIIM chamber and the fourth column excludes the BIPM chamber. The uncertainty on the BIPM data was taken to be 0.17% for the purpose of these calculations. The cylindrical approximation to the LPRI was used here.

Quantity	Original	Revised		
		all	exclude VNIIM	exclude VNIIM, BPIM
Mean	1.0010	1.0053	1.0048	1.0052
RMS deviation	0.0019	0.0032	0.0027	0.0024
Weighted mean	1.0016	1.0048	1.0043	1.0052
χ^2	9.47	23.03	14.82	6.98
χ^2/df	0.63	1.54	1.06	0.54
p	0.85	0.08	0.39	0.90

Table 8: Comparison of the ^{137}Cs Monte Carlo $K_{\rm wall}$ values obtained with EGSnrc with those reported by the BIPM and other sources.

Lab	$K_{\rm wall}^{\rm MC}$	$K_{\rm wall} = K_{\rm at}K_{\rm sc}K_{\rm cep}$	ref	%Δ
GUM	1.02781(17)	1.0158	[2]	1.177
LNMRI	1.02749(17)	1.0157	[2]	1.156
OMH	1.02874(13)	1.0166	[2]	1.191
BIPM pancake	0.99993(6)	1.0022	[30]	-0.227
BIPM 122	1.02749(17)	1.0157	[2]	1.156
NIST-1	1.02945(16)	1.0189	[33]	1.035
NIST-50	1.03613(7)	1.0262	[33]	0.968

Table 9: Comparison of the ^{137}Cs Monte Carlo $K_{\rm an}$ axial non-uniformity values obtained with EGSnrc with those reported by BIPM and other sources. The values were calculated by dividing the parallel beam value by the point source value.

Lab	dose$\times K_{\rm wall}^{\rm MC,point}$ $\times 10^{-12}$Gy	dose$\times K_{\rm wall}^{\rm MC,parallel}$ $\times 10^{-12}$Gy	$K_{\rm an}^{\rm MC}$	$K_{\rm an}^{\rm NMI}$	ref	%Δ
GUM	2.8640(8)	2.8648(11)	1.0003(5)	1.0000	[2]	0.030
LNMRI	2.8614(11)	2.8617(11)	1.0001(6)	1.0000	[2]	0.010
OMH	2.8670(11)	2.8643(11)	0.9991(6)	0.9998	[2]	-0.070
BIPM pancake	2.8587(6)	2.8638(9)	1.0018(4)	0.9981	[30]	0.370
BIPM 122	2.8614(11)	2.8617(11)	1.0001(4)	1.0000	[2]	0.010
NIST-1	2.8620(9)	2.8586(14)	0.9988(6)	1.0000	[33]	-0.120
NIST-50	2.8649(9)	2.8643(9)	0.9998(4)	1.0000	[33]	-0.020

Table 10: Revised values of comparison results for ^{137}Cs after correcting both the NMI and BIPM air-kerma rates to use the Monte Carlo calculated values of $K_{\rm wall}$ and $K_{\rm an}$. All corrections were made relative to the BIPM pancake chamber.

Lab	$\left(\frac{K_{\rm lab}}{K_{\rm BIPM}}\right)_{\rm orig}$	$\Delta K_{\rm wall}$	$\Delta K_{\rm an}$	$\left(\frac{K_{\rm lab}}{K_{\rm BIPM}}\right)_{\rm revised}$
GUM	0.9914	1.01177	1.00030	1.0019
LNMRI	0.9915	1.01156	1.00010	1.0016
OMH	0.9954	1.01191	0.99930	1.0056
BIPM pancake	1.0000	0.99773	1.00370	1.0000
BIPM 122	0.9932	1.01156	1.00010	1.0034
NIST[a]	1.0017	1.010	.9993	1.0110

[a] averaging for the two chambers. Comparison from [25].

8 Figures

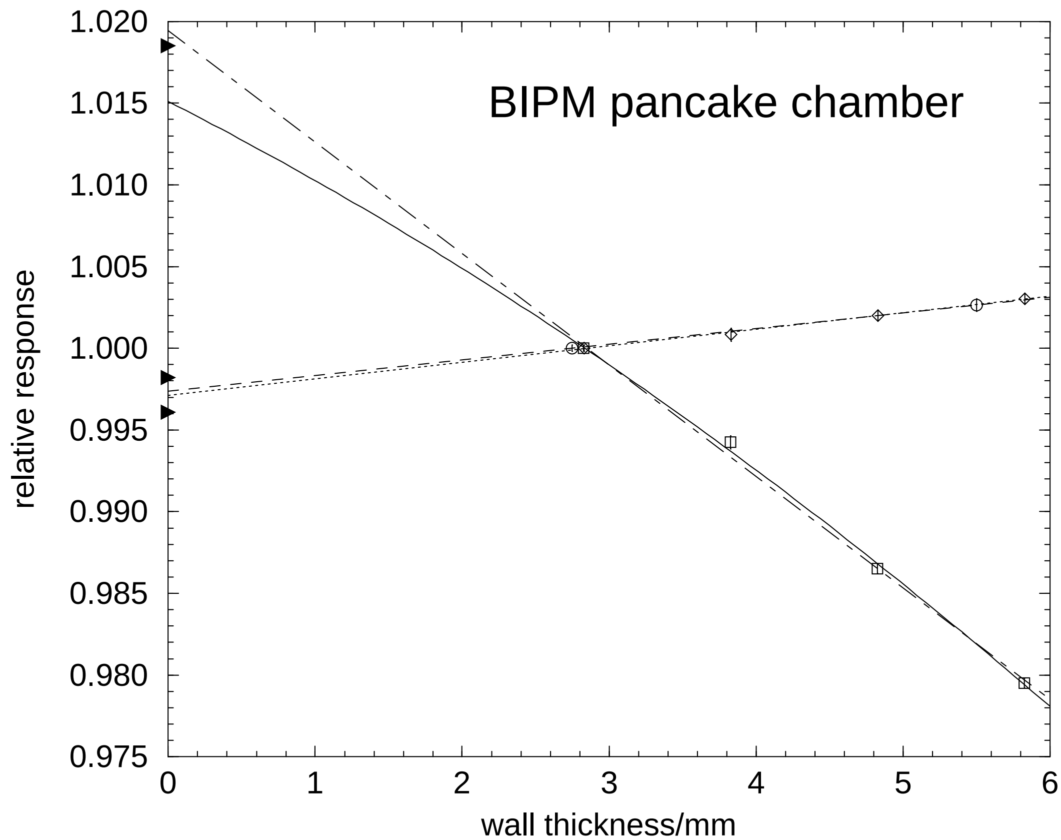

Figure 1: Response vs. wall thickness extrapolations for the BIPM pancake chamber. The squares are the data obtained for increasing front wall thickness; these data points fit best to a parabola, as noted by Boutillon and Niatel [18] but the uncertainty on the extrapolation is very large for the Monte Carlo data. The parabola and straight line fits are shown. The two data sets for the side and back walls (circles and diamonds, respectively) lie virtually on top of each other. The BIPM's original extrapolated results [18] are marked by the triangles on the y-axis (see also table 3). All data points are normalized to 1.00 for the chamber's real wall thickness in the direction considered (just under 3 mm in all 3 cases).

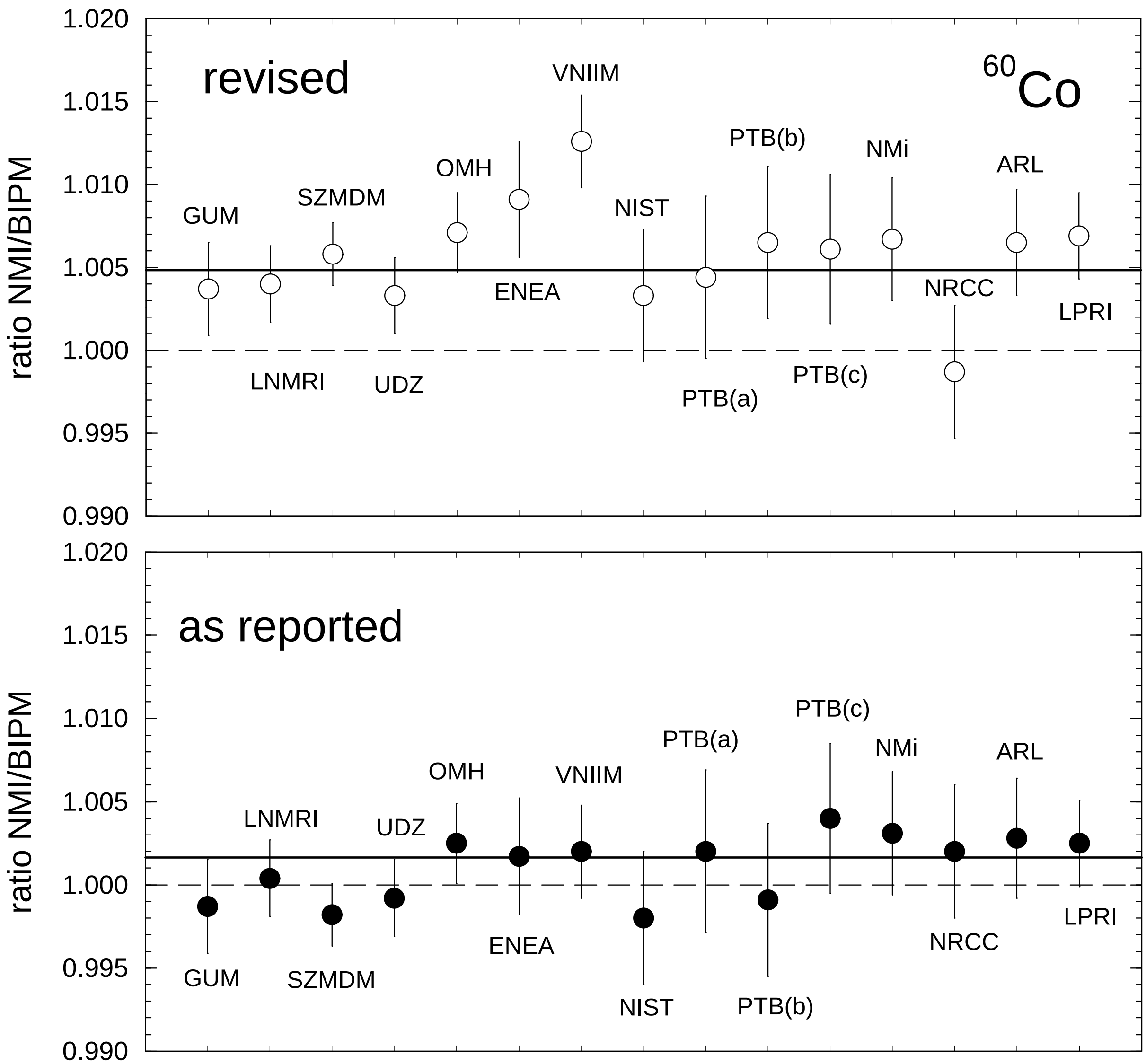

Figure 2: The "as reported" ratios of air-kerma rates of various NMI's at the BIPM and the same results after applying both the K_{wall} and K_{an} corrections as obtained from Monte Carlo calculations. Note that not only has the average value gone up with the revised values, but there is a change in the baseline of the BIPM of either 0.33% or 0.46%. Note that the cylindrical approximation to the LPRI is shown here.

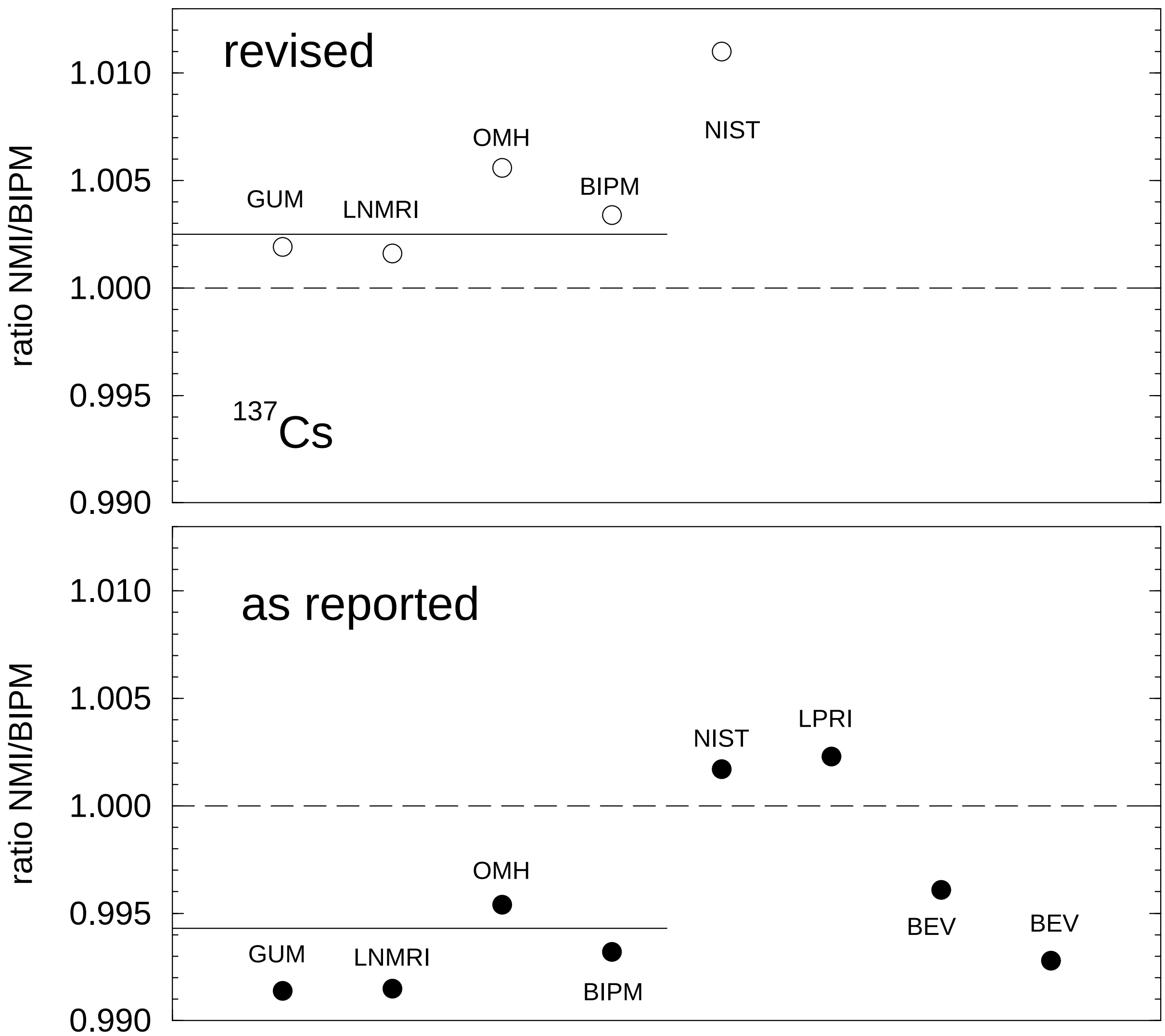

Figure 3: The "as reported" ratios of air-kerma rates of various NMI's at the BIPM for ^{137}Cs and the same results after applying both the $K_{\rm wall}$ and $K_{\rm an}$ corrections as obtained from Monte Carlo calculations. Note that not only has the average value gone up with the revised values, but there is a change in the baseline of the BIPM of 0.14%. The solid lines show the weighted averages for just the CC01 chambers analysed by Boutillon[2].

References

[1] A. F. Bielajew and D. W. O. Rogers. Implications of new correction factors on primary air kerma standards in ^{60}Co beams. *Phys. Med. Biol.*, 37:1283 – 1291, 1992.

[2] M. Boutillon. About the determination of the wall correction in cavity chambers. *BIPM Report CCRI(I)/99 – 3*, page 10 pages, 1999.

[3] D. W. O. Rogers and A. F. Bielajew. Wall attenuation and scatter corrections for ion chambers: measurements versus calculations. *Phys. Med. Biol.*, 35:1065 – 1078, 1990.

[4] A. F. Bielajew. On the technique of extrapolation to obtain wall correction factors for ion chambers irradiated by photon beams. *Med. Phys.*, 17:583 – 587, 1990.

[5] D. W. O. Rogers, A. F. Bielajew, and A. E. Nahum. Ion chamber response and $A_{\rm wall}$ correction factors in a ^{60}Co beam by Monte Carlo simulation. *Phys. Med. Biol.*, 30:429 – 443, 1985.

[6] A. F. Bielajew, D. W. O. Rogers, and A. E. Nahum. Monte Carlo simulation of ion chamber response to ^{60}Co – Resolution of anomalies associated with interfaces. *Phys. Med. Biol.*, 30:419 – 428, 1985.

[7] A. F. Bielajew. Ionization cavity theory: a formal derivation of perturbation factors for thick-walled ion chambers in photon beams. *Phys. Med. Biol.*, 31:161 – 170, 1986.

[8] D. W. O. Rogers, A. F. Bielajew, N. V. Klassen, C. K. Ross, J. P. Seuntjens, K. R. Shortt, and L. Van der Zwan. NRC Activities and Publications, 1995–1997: Report to CCEMRI(I) Meeting, BIPM. *CCEMRI(1)97–29*, 1997.

[9] K. R. Shortt, A. F. Bielajew, C. K. Ross, M. J. Corsten, J. T. Burke, P. R. S. Howard, and D. C. Marchington. Determination of $A_{\rm wall}$ corrections using a non-linear extrapolation to zero-wall thickness. *Med. Phys. (abstract)*, 23:1139, 1996.

[10] F. Delaunay, B. Chauvenet, and J. P. Simoën. Caracterisation primaire en debit de kerma dans l'air faisceau de ^{60}Co nIIB. Note Technique LPRI/93/013, Laboratoire Primaire des Rayonnements Ionisants, Gif-sur-Yvette, France, 1993.

[11] S. Kondo and M. L. Randolph. Effect of finite size of ionization chambers on measurements of small photon sources. *Radiat. Res.*, 13:37 – 60, 1960.

[12] A. F. Bielajew. An analytic theory of the point-source non-uniformity correction factor for thick-walled ionisation chambers in photon beams. *Phys. Med. Biol.*, 35:517 – 538, 1990.

[13] A. F. Bielajew. Correction factors for thick-walled ionisation chambers in point-source photon beams. *Phys. Med. Biol.*, 35:501 – 516, 1990.

[14] H. Tölli, A. F. Bielajew, O. Mattsson, G. Sernbo, and K. A. Johansson. Fluence non-uniformity effects in air kerma determination around brachytherapy sources. *Phys. Med. Biol.*, 42:1301 – 1318, 1997.

[15] I. Kawrakow. Accurate condensed history Monte Carlo simulation of electron transport. I. EGSnrc, the new EGS4 version. *Med. Phys.*, 27:485 – 498, 2000.

[16] I. Kawrakow. Accurate condensed history Monte Carlo simulation of electron transport. II. Application to ion chamber response simulations. *Med. Phys.*, 27:499 – 513, 2000.

[17] D. W. O. Rogers. Fundamentals of High Energy X-ray and Electron Dosimetry Protocols. In J. Purdy, editor, *Advances in Radiation Oncology Physics, Medical Physics Monograph 19*, pages 181 – 223. AAPM, New York, 1992.

[18] M. Boutillon and M-T. Niatel. A Study of a Graphite Chamber for Absolute Exposure Measurements of ^{60}Co Gamma Rays. *Metrologia*, 9:139 – 146, 1973.

[19] M.-T. Niatel, T. P. Loftus, and W. Oetzmann. Comparison of Exposure Standards for ^{60}Co Gamma Rays. *Metrologia*, 11:17 – 23, 1975.

[20] W. R. Nelson, H. Hirayama, and D. W. O. Rogers. The EGS4 Code System. Report SLAC–265, Stanford Linear Accelerator Center, Stanford, California, 1985.

[21] M. S. MacPherson, C. K. Ross, and D. W. O. Rogers. Accurate Measurements of the Collision Stopping Powers for 5 to 30 MeV Electrons. *Med. Phys. (abs)*, 25:A104, 1998.

[22] D. W. O. Rogers, G. M Ewart, A. F. Bielajew, and G. van Dyk. Calculation of Electron Contamination in a ^{60}Co Therapy Beam. *in "Proceedings of the IAEA International Symposium on Dosimetry in Radiotherapy" (IAEA, Vienna), Vol 1*, pages 303 – 312, 1988.

[23] P. R. Almond, P. J. Biggs, B. M. Coursey, W. F. Hanson, M. S. Huq, R. Nath, and D. W. O. Rogers. A status report on the absorbed dose to water based beam calibration protocol under consideration by the AAPM. Report to IAEA committee of consultants, TG–51, 1996.

[24] P. J. Allisy-Roberts, J. F. Boas M. Boutillon, and R. B. Huntley. Comparison of the air kerma standards of the ARL and the BIPM for ^{60}Co γ rays. *BIPM Report BIPM–98/4*, 1998.

[25] A. Leitner, J. Witzani, M. Boutillon, P. Allisy-Roberts, F. Delaunay, E. Leroy, P. Lamperti, C. Strachotinsky, and I. Csete. International comparison of air kerma standards in 137Cs gamma radiation. *Metrologia*, 34:169 – 175, 1997.

[26] P. J. Allisy-Roberts, M. Boutillon, Z. Referowski, and N. Paz. Comparison of the standards of air kerma of the GUM and the BIPM for ^{60}Co γ rays. *BIPM Report BIPM–97/2*, 1997.

[27] P. J. Allisy-Roberts, M. Boutillon, and L. N. Rodrigues. Comparison of the standards of air kerma of the LNMRI and the BIPM for ^{60}Co γ rays. *BIPM Report BIPM–96/3*, 1996.

[28] A. M. Perroche and V. Spasić Jokić. Comparison of the air kerma standards of SZMDM and BIPM for ^{60}Co radiation. *BIPM Report BIPM–92/3*, 1992.

[29] A. M. Perroche, M. Boutillon, I. Kovar, and R. Wagner. Comparison of the air kerma standards of the UDZ and the BIPM for ^{60}Co radiation. *BIPM Report BIPM–93/1*, 1993.

[30] A. M. Perroche, M. Boutillon, and I. Csete. Comparison of the air kerma standards of the OMH and the BIPM for ^{137}Cs and ^{60}Co γ rays. *BIPM Report BIPM–94/13*, 1994.

[31] M. P. Toni R. F. Laitano. The primary exposure standard for ^{60}Co gamma radiation: characteristics and measurements procedures. *ENEA Report RT/PROT(83)28*, 1983.

[32] P. J. Allisy-Roberts, M. Boutillon, A. V. Oborin N. D. Villevalde, and E. N. Yurjatin. Comparison of the standards of air kerma of the VNIIM and the BIPM for ^{137}Cs and ^{60}Co γ rays. *BIPM Report BIPM–98/3*, 1998.

[33] T. P. Loftus and J. T. Weaver. Standardization of ^{60}Co and ^{137}Cs Gamma-Ray Beams in Terms of Exposure. *J. Res. Nat. Bur. Stand.*, 78A:465 – 476, 1974.

[34] A. M. Perroche, M. Boutillon, J. Daures, A. Ostrowsky F. Delaunay, E. Leroy, and B. Chauvenet. Comparison of the standards of air kerma and of absorbed dose of the LPRI and the BIPM for ^{60}Co γ rays. *BIPM Report BIPM–94/6*, 1994.

Appendix: Figures showing calculated extrapolation

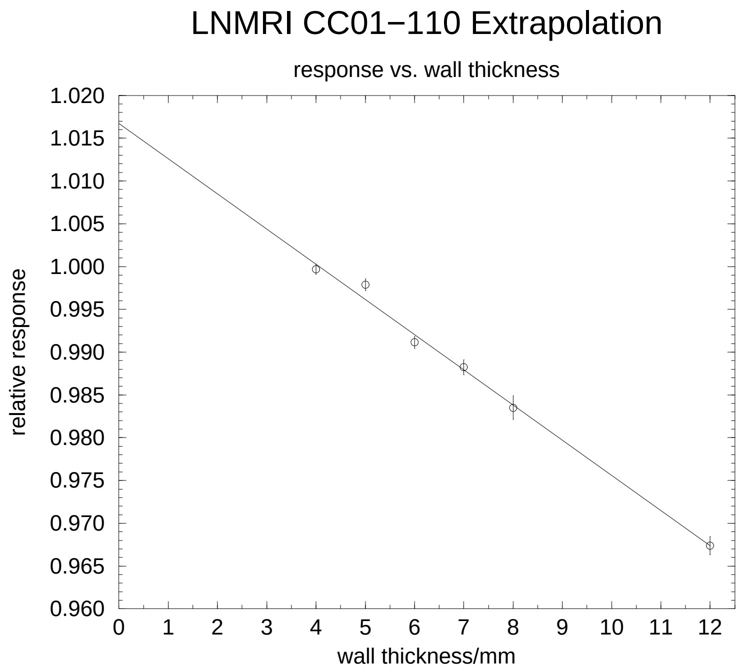

Figure 4: Response vs. wall thickness extrapolation for the LNMRI chamber.

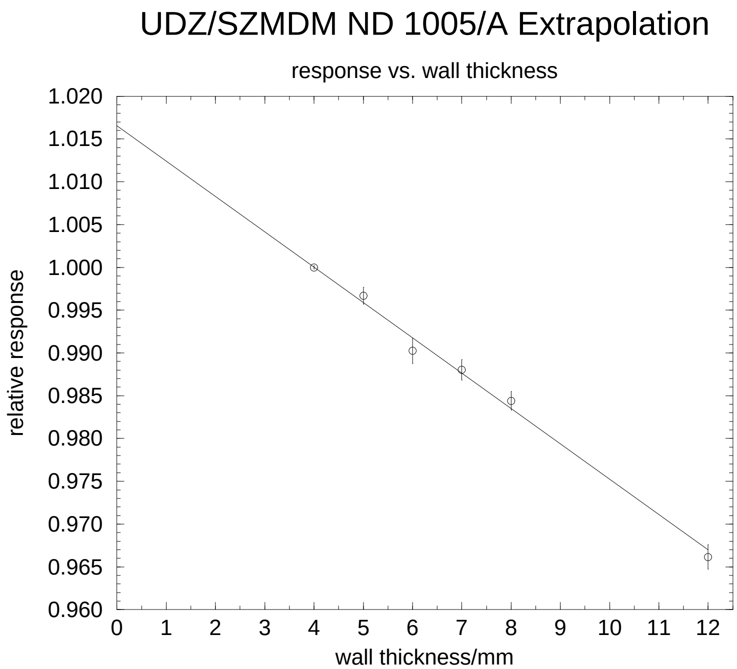

Figure 5: Response vs. wall thickness extrapolation for the UDZ and SZMDM chambers.

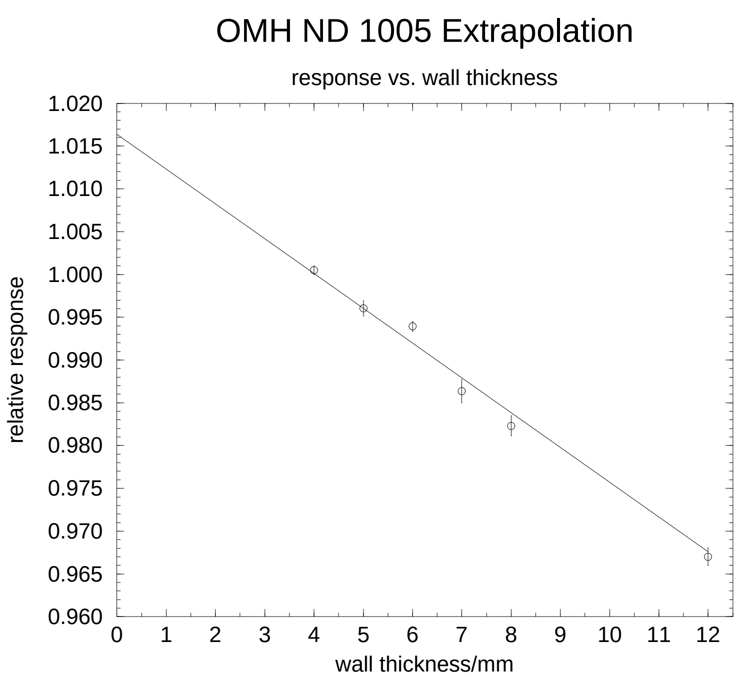

Figure 6: Response vs. wall thickness extrapolation for the OMH and ENEA chambers.

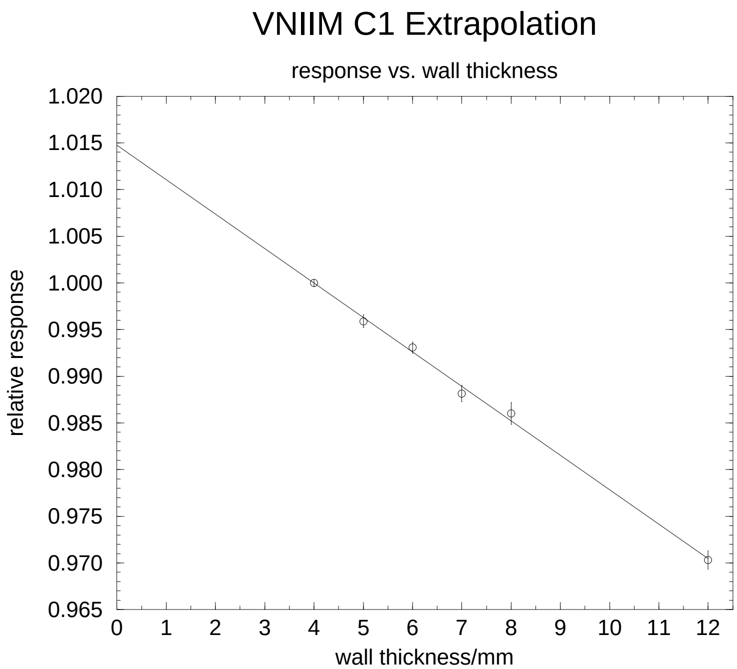

Figure 7: Response vs. wall thickness extrapolation for the VNIIM C1 chamber.

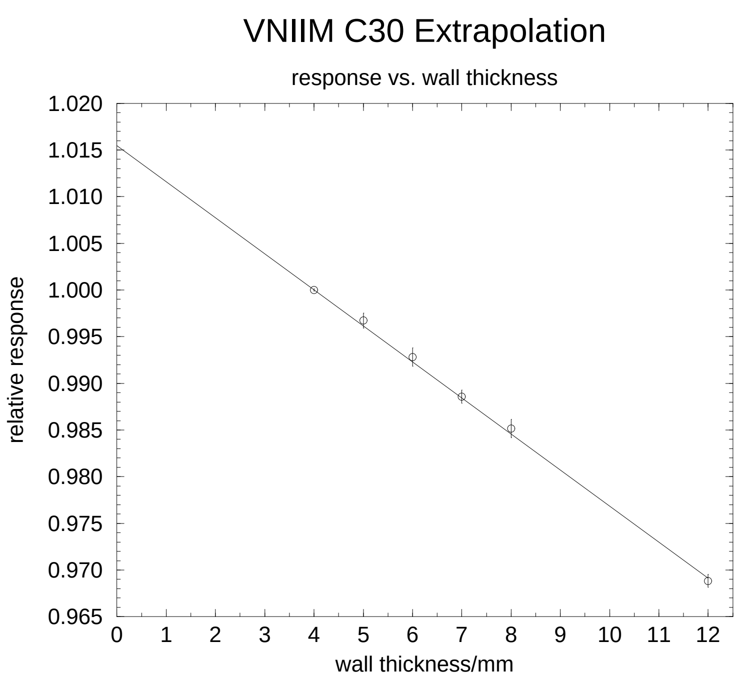

Figure 8: Response vs. wall thickness extrapolation for VNIIM C30 chamber.

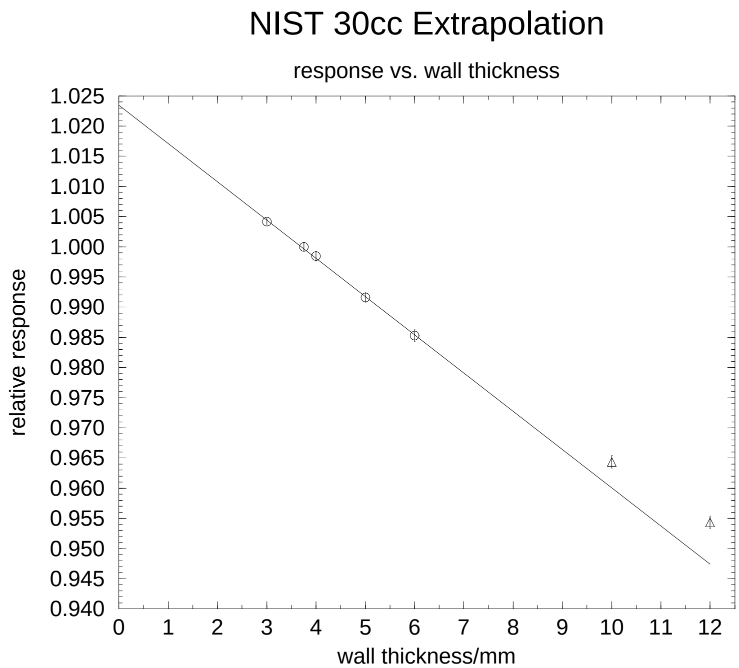

Figure 9: Response vs. wall thickness extrapolation for the NIST 30cc chamber. The open circles represent the data used to obtain the fit for the extrapolation.

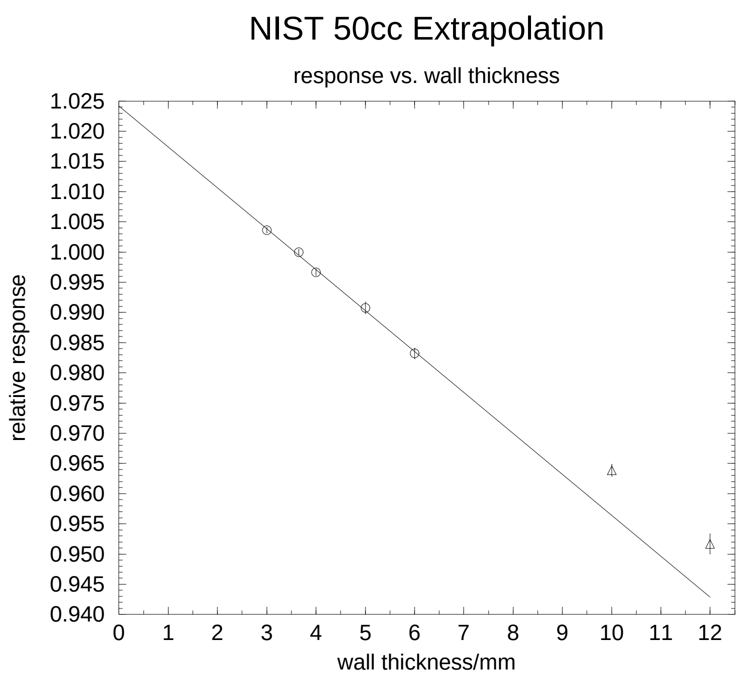

Figure 10: Response vs. wall thickness extrapolation for the NIST 50cc chamber. The open circles represent the data used to obtain the fit for the extrapolation.

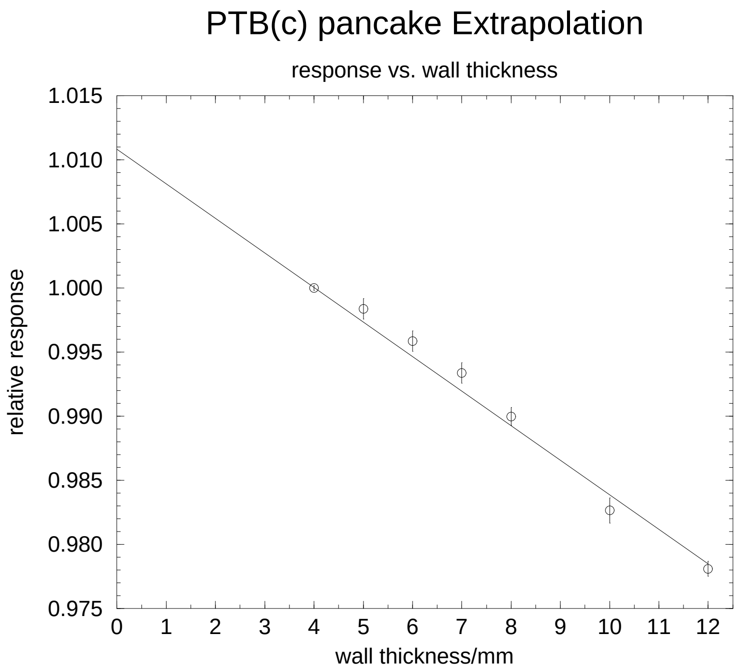

Figure 11: Response vs. wall thickness extrapolation for the PTB pancake chamber (c).

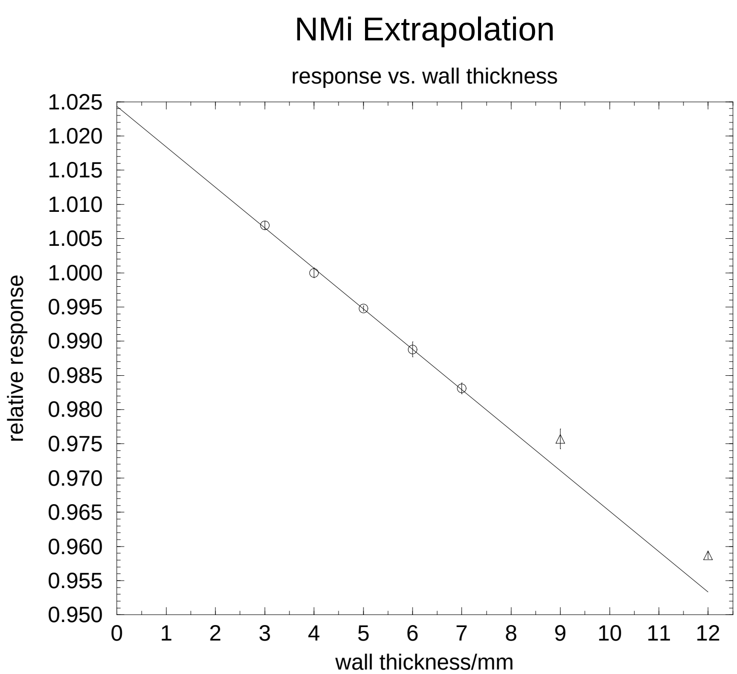

Figure 12: Response vs. wall thickness extrapolation for the NMi chamber. The open circles represent the data used to obtain the fit for the extrapolation.

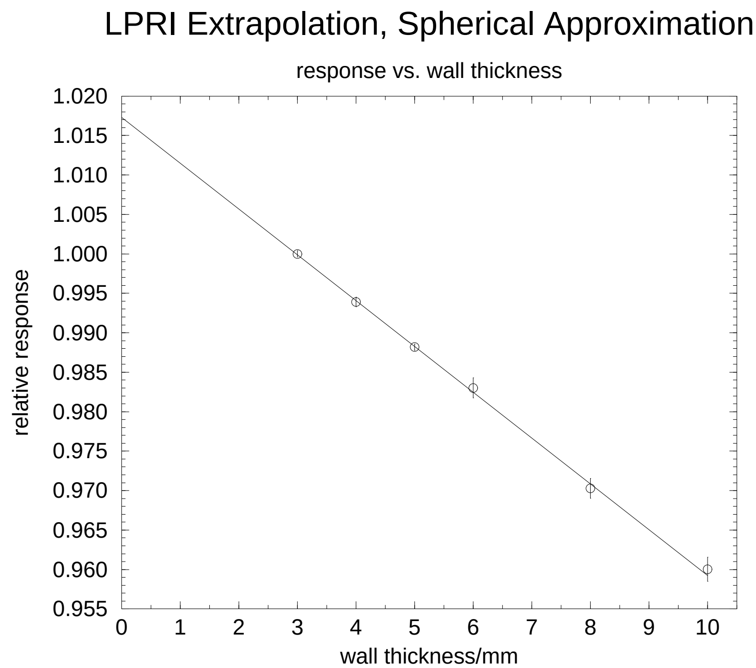

Figure 13: Response vs. wall thickness extrapolation for the LPRI chamber approximated as a sphere.

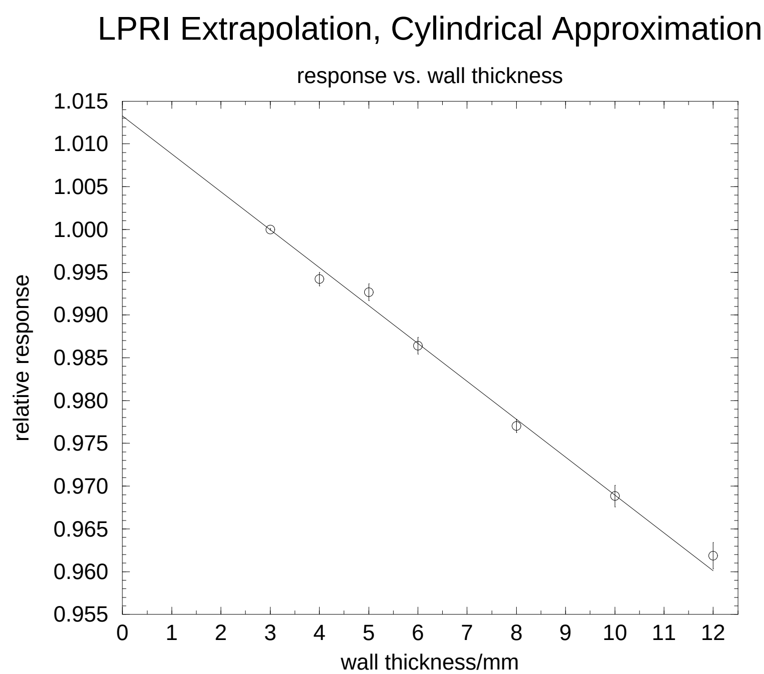

Figure 14: Response vs. wall thickness extrapolation for the LPRI chamber approximated as a cylinder.